Eur. Phys. J. D **39**, 277–282 (2006)
DOI: 10.1140/epjd/e2006-00103-6

THE EUROPEAN PHYSICAL JOURNAL D

Quantum entanglement and classical bifurcations in a coupled two-component Bose-Einstein condensate

Q. Xie[1] and W. Hai[1,2,a]

[1] Department of physics, Hunan Normal University, Changsha 410081, P.R. China
[2] Laboratory of Magnetic Resonance and Atomic and Molecular Physics, Wuhan Institute of Physics and Mathematics, The Chinese Academy of Sciences, Wuhan 430071, P.R. China

Received 6 November 2005 / Received in final form 18 January 2006
Published online 18 May 2006 –

Abstract. We investigate the relation between quantum states and classical fixed-point bifurcations in a coupled two-component Bose-Einstein condensate (BEC). It is shown that the classical bifurcations are closely related to a topological change of the corresponding quantum levels, and such a structure change can be manifested in the entanglement properties of the corresponding quantum states. That is, the entanglement of the quantum states displays some peaks near the classical bifurcation points.

PACS. 03.75.Gg Entanglement and decoherence in Bose-Einstein condensates – 03.67.Mn Entanglement production, characterization, and manipulation – 05.30.Jp Boson systems – 05.40.-a Fluctuation phenomena, random processes, noise, and Brownian motion

Quantum entanglement, as one of the most striking features of quantum theory, is now regarded as a valuable resource that can be exploited to implement many useful tasks in quantum information science [1]. Apart from its practical applications, studies of the entanglement characteristics of various interacting systems have shed new insight into fundamental aspects of quantum physics. Recently, a great deal of effort has been devoted to understanding the impact of quantum phase transitions (QPTs) on quantum entanglement [2–7]. In addition, there have been attempts to relate chaos and localization to entanglement [8,9]. Therefore, quantum entanglement has provided a very useful tool to reexamine some well-understood properties of complex many-body systems.

A QPT represents a qualitative change of the ground state when a control parameter is changed across a critical point. While in the classical version, a stationary solution of minimal energy corresponds to a stable fixed point. As the parameter is varied to a special value, the original fixed point may lose its stability and some new unstable fixed points may appear. Such a phenomenon was known as the dynamical bifurcation. Thus it is natural to ask how the classical critical behavior of a system can affect the quantum entanglement. Schneider and Milburn first alluded to such a link in the Dicke model [10]. They argued that the ground state entanglement reaches a maximal value at a classical bifurcation point. Then Hines and coworkers extended such an investigation to Jahn-Teller models and coupled giant spins models exhibiting one exactly supercritical pitchfork bifurcation [11,12]. It is demonstrated that when a fixed point undergoes a supercritical pitchfork bifurcation, the ground state achieves its maximum amount of entanglement near the classical critical point. The authors further conjectured that this will be a generic feature of the systems whose classical limit exhibits such a bifurcation. More recently, Hou et al. discussed the influence of this bifurcation on both static and dynamical entanglement in an integrable quantum dimer model [13]. It is pointed out that the highest excited state entanglement instead of the ground state entanglement displays a peak near the bifurcation point, and the mean entanglement, defined to be averaged over time, exhibits a maximum near the classical bifurcation point. These seem to mean that the entanglement behavior near and at the bifurcation points depends on the studied models. Therefore, it would be interesting to understand in more detail the entanglement properties of systems where different types of bifurcations can be found.

In this brief note, we use a coupled two-component or two-state Bose-Einstein condensate (BEC) as an example to revisit the connection between the entanglement state and bifurcation. The Hamiltonian takes the well known form [13–16,18,19,21–27]: $\hat{H} = \frac{\gamma}{2}(\hat{a}^\dagger\hat{a} - \hat{b}^\dagger\hat{b}) + \frac{c}{2}(\hat{a}^\dagger\hat{b} + \hat{a}\hat{b}^\dagger) + \frac{u}{4}(\hat{a}^\dagger\hat{a} - \hat{b}^\dagger\hat{b})^2$, where generators and annihilators $\hat{a}^\dagger, \hat{a}$ and $\hat{b}^\dagger, \hat{b}$ are for two different quantum states. In the Hamiltonian $\hat{H}$, γ is the energy offset between the two quantum states. The parameter c measures the coupling between the two states while u is the interacting strength between bosons. The parameter u can be positive or negative depending on the mixture of different components in the spinor BECs [15]. In this system the total number of

[a] e-mail: adcve@public.cs.hn.cn

bosons N is conserved. We also notice that the quantum dimer model considered in reference [13] corresponds formally to a special case of $\gamma = 0$ and $u = 2.0$ in our model. We find two different types of bifurcation existing in this system: one is the saddle-node bifurcation and the other the supercritical pitchfork bifurcation. Our results show that the classical bifurcations are closely associated with a topological change in the structure of the corresponding quantum energy levels. The saddle-node bifurcation, induced by the change of the energy offset γ, is related to the avoided level-crossing. While for a vanishing $\gamma = 0$, the change of the ratio of $\lambda/c = (N-1)u/c$ causes the supercritical pitchfork bifurcation linked to the near degeneracy of the structure of quantum energy levels. And these changes in the structure of the quantum energy levels and thus the classical bifurcations can be reflected in the entanglement properties, that leads to some entanglement peaks near the classical bifurcation points.

We now begin to derive the corresponding classical dynamics. Following reference [14], we introduce the angular momentum operator $\hat{J}$ in terms of the two boson modes

$$\hat{J}_x = \frac{1}{2}(\hat{a}^\dagger\hat{b} + \hat{b}^\dagger\hat{a}),\ \hat{J}_y = \frac{i}{2}(\hat{b}^\dagger\hat{a} - \hat{a}^\dagger\hat{b}),\ \hat{J}_z = \frac{1}{2}(\hat{a}^\dagger\hat{a} - \hat{b}^\dagger\hat{b}), \tag{1}$$

for which the Casimir invariant is $\hat{J}^2 = (N/2)(N/2+1)$. The Hamiltonian of the system can thus be of a simple form

$$\hat{H} = \gamma\hat{J}_z + u\hat{J}_z^2 + c\hat{J}_x. \tag{2}$$

It is convenient to choose the simultaneous eigenstates of $\hat{J}^2$ and $\hat{J}_z$ as a basis defined by

$$\hat{J}^2|j,m\rangle = j(j+1)|j,m\rangle, \hat{J}_z|j,m\rangle = m|j,m\rangle, \tag{3}$$

where

$$|j,m\rangle = \frac{(\hat{a}^\dagger)^{N/2+m}(\hat{b}^\dagger)^{N/2-m}}{\sqrt{(N/2+m)!(N/2-m)!}}|vac\rangle. \tag{4}$$

Here the values of m range from $-N/2$ to $N/2$ and $j = N/2$, and $|vac\rangle$ denotes the vacuum state. To obtain the corresponding classical dynamics, we use a generalized spin coherent state (SCS) as the initial state, which minimizes the initial uncertainty product, so that the mean values of some physical quantities have the correspondence in classical phase space. Such a state may be defined by [17]

$$|\theta,\phi\rangle = \exp\left[-i\theta(J_x\sin\phi - iJ_y\cos\phi)\right]|j,-j\rangle. \tag{5}$$

Utilizing these useful relations $\langle\theta,\phi|\hat{J}_z|\theta,\phi\rangle = -j\cos\theta$, $\langle\theta,\phi|\hat{J}_z^2|\theta,\phi\rangle = j(j-1/2)\cos^2\theta + j/2$ and $\langle\theta,\phi|\hat{J}_x|\theta,\phi\rangle = j\sin\theta\cos\phi$, we obtain the corresponding classical Hamiltonian (up to a trivial constant)

$$H_{cl} = \langle\theta,\phi|\hat{H}|\theta,\phi\rangle/j = \gamma z - \frac{1}{2}\lambda z^2 + c\sqrt{1-z^2}\cos\phi, \tag{6}$$

where $z = -\cos\theta$ denotes the population difference between the two internal states and ϕ the relative phase, and $\lambda = (N-1)u$. If we use the the population difference z and relative phase ϕ as the classical canonical variables, the equations of motion are given by the classical Hamiltonian as [14,16]

$$\dot{z} = c\sqrt{1-z^2}\sin\phi, \tag{7}$$

$$\dot{\phi} = \gamma + \lambda z - c\frac{z}{\sqrt{1-z^2}}\cos\phi, \tag{8}$$

which are similar to that for the condensates in a double-well potential [18,19]. We have investigated such a system in mean field mechanism [20]. One distinct difference between the two models is the sign of the parameter u. For the case of condensates in a double-well potential, the sign is just determined by the sign of the scattering length, but for our case the sign is determined by the mixture of different components in the real spinor BEC [15].

Because bifurcations are often accompanied by a loss of stability and the appearance of new fixed points, one can explore the bifurcation behavior by analyzing the change of the number of the corresponding fixed points or stationary states [21–24]. The stationary state solutions of equations (7) and (8) can be determined from $dz/dt = 0$ and $d\phi/dt = 0$. In the region $[0, 2\pi)$ of the relative phase, we find two different modes of stationary states in the system: one is the equal-phase mode with zero relative phase $\phi = 0$, and the other the anti-phase mode with the relative phase $\phi = \pi$. Small oscillations around those stationary states with nonzero the population difference z are macroscopic quantum self-trapping (MQST) states [18,19]. If the MQST states only oscillate around $dz/dt = 0$, running-phase MQST states appear. On the other hand, many novel features have been revealed in this system through bifurcation, including the nonlinear Landau-Zener tunneling [23] and hysteresis [24]. The number of fixed points mainly depends on the ratios γ/c, λ/c and the relative phase. For the equal-phase mode, only one stable fixed point exists for $\lambda/c \leq 1$. When $\lambda/c > 1$, there are two stable fixed points and one unstable fixed point for $(\lambda/c)^{2/3} - (\gamma/c)^{2/3} > 1$, and only one stable fixed point exists for $(\lambda/c)^{2/3} - (\gamma/c)^{2/3} < 1$. Saddle-node bifurcations occur at the points satisfying $(\lambda/c)^{2/3} - (\gamma/c)^{2/3} = 1$. For the anti-phase mode, the parametric dependence of fixed points and stationary states is very different. When $\lambda/c \geq -1$, only one fixed point appears and it is stable. When $\lambda/c < -1$, two stable and one unstable fixed points exist for $(\lambda/c)^{2/3} - (\gamma/c)^{2/3} > 1$ and only one stable fixed point emerges for $(\lambda/c)^{2/3} - (\gamma/c)^{2/3} < 1$. Saddle-node bifurcations also occur at the points satisfying $(\lambda/c)^{2/3} - (\gamma/c)^{2/3} = 1$. The saddle-node bifurcation is fundamental in the study of nonlinear system, since this is one of the most basic processes by which a pair of periodic orbits are created, one of them is always unstable (the saddle), while the other periodic orbit is always stable (the node). From the above analysis, we can see that the system will show various different forms of saddle-node bifurcations depending on different system parameters. The fixed points of this classical system correspond to the eigenstates of the quantum Hamiltonian, which can be expanded in terms of Fock states (see Eq. (11)). At a

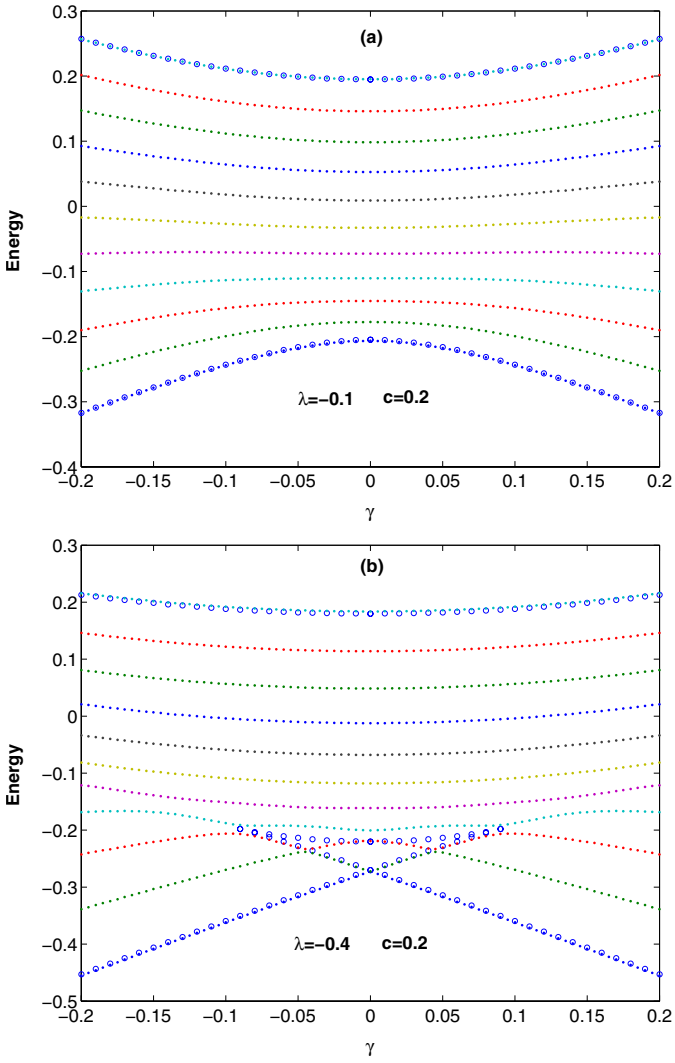

Fig. 1. (Color online) Energy levels from the quantum model $\hat{H}$ ($N = 10$) and the classical Hamiltonian H_{cl} for (a) $\lambda/c = -0.5$ and (b) $\lambda/c = -2$. The dot lines are quantized energy levels; the open circles are classical energy levels. Compared with the classical energy, the quantized energy levels from $\hat{H}$ have been divided by $N/2$.

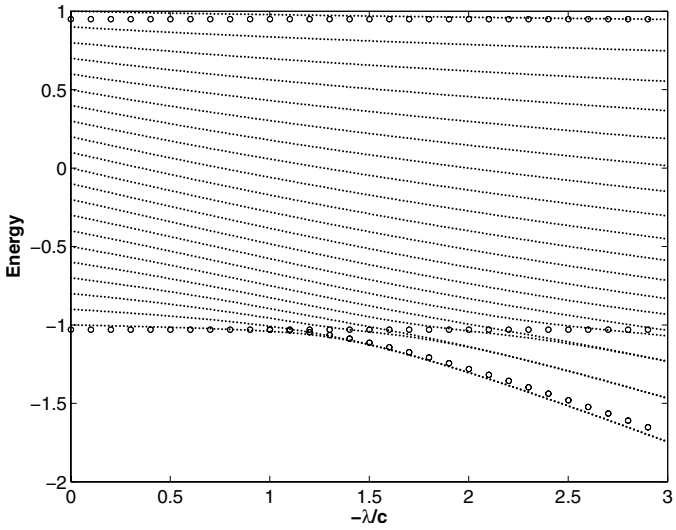

Fig. 2. Energy levels from the quantum model $\hat{H}$ ($N = 20$) and the classical Hamiltonian H_{cl}. The dot lines are quantized energy levels; the open circles are classical energy levels. Compared with the classical energy, the quantized energy levels from $\hat{H}$ have been divided by $N/2$.

fixed number of bosons N, the quantum Hamiltonian becomes a $(N+1)\times(N+1)$ matrix and then the quantum states can be numerically calculated. Here we consider the case where the parameter u is taken as negative value, so that the classical bifurcations are related to the lower part of the quantum energy levels, only including the ground state and a few low excited states. Figure 1 shows the classical energy and the corresponding quantum energy structures as functions of γ. Clearly, there is a drastic change in the structure of energy levels as the interaction strength λ changes: a net of anti-crossings appearers in the lower part of the quantized energy levels when $\lambda/c < -1$. In particular, the classical energy levels (a loop structure) envelop the net anti-crossings in the quantum energy levels, also discussed in depth in references [25,26].

For the case $\gamma = 0$, the supercritical pitchfork bifurcation will occur. This type of bifurcation is common in physical problems that have a symmetry. For the equal-phase mode, only one stable fixed point $z = 0$ exists if $\lambda/c < 1$, and two new stable fixed points $z_\pm = \pm\sqrt{1-(\lambda/c)^{-2}}$ appear if $\lambda/c > 1$ accompanied by a loss of stability of the original one $z = 0$. This means a supercritical pitchfork bifurcation takes place at $\lambda/c = 1$. However, for the anti-phase mode, the supercritical pitchfork bifurcation occurs at $\lambda/c = -1$. There is only one stable fixed point $z = 0$ for $\lambda/c > -1$ and two stable fixed points $z_\pm = \pm\sqrt{1-(\lambda/c)^{-2}}$ with an unstable one $z = 0$ for $\lambda/c < -1$. Figure 2 shows the classical energy and the corresponding quantum energy structures as functions of $-\lambda/c$. Obviously, as the ratio $-\lambda/c$ increases, the ground state and the first excited state of the quantum system become nearly degenerate, while the classical descriptions experience the supercritical pitchfork bifurcation. Figure 3 refers to the energy gap between the lowest two eigen-energies in the quantum Hamiltonian as a function of the ratio $-\lambda/c$. It can be inferred that as $N \to \infty$, the quantum nearly degenerate point approaches the classical bifurcation points $-\lambda/c = 1$.

Many particle entanglement have been widely studied in this system, which allows to investigate the boundary between quantum physics and classical physics [14]. For instance, it has been shown that the coherent interactions in a BEC allow to generate many-particle entanglement [28]. We now employ the entropy of subsystem as a measure of the quantum entanglement [27] to discuss the relation between the quantum states and the classical bifurcations. More precisely, we will use the von Neumann entropy of the reduced density operator of any subsystem. The reduced density operator of a subsystem is achieved

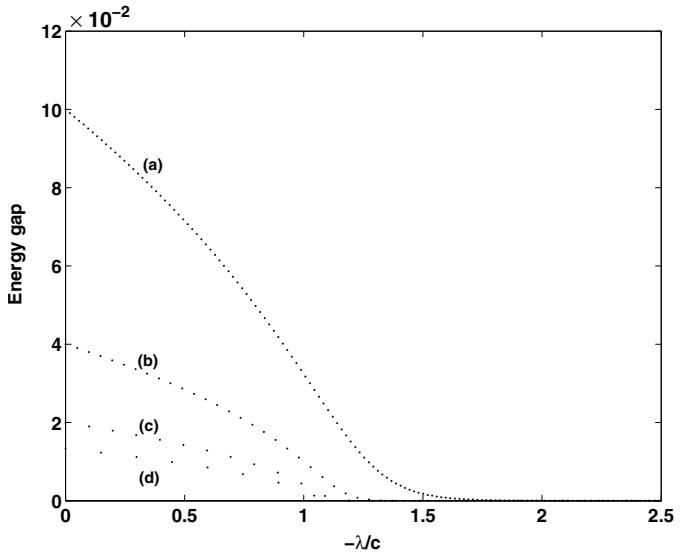

Fig. 3. Energy gap between the lowest two eigen-energies in the quantum Hamiltonian at $\gamma = 0$. The total number N is (a) $N = 20$, (b) $N = 50$, (c) $N = 100$, (d) $N = 150$, respectively.

by tracing out the other subsystem via the partial trace. Once we obtain the reduce density matrix, the entanglement can be readily calculated. If ρ_{ab} is the density operator describing some states of a bipartite system, the reduced density operator for subsystem a is defined by

$$\rho_a = \mathrm{Tr}_b\left(\rho_{ab}\right) \tag{9}$$

where Tr_b is the partial trace over subsystem b. The entropy of entanglement is then written as

$$E(\rho_a) = -\mathrm{Tr}\left(\rho_a \log\left(\rho_a\right)\right) = -\sum_k \lambda_k \log\left(\lambda_k\right) \tag{10}$$

where the logarithm is taken in base 2, and $\{\lambda_k\}$ are the set of eigenvalues of the reduced density operator ρ_a. The value of E varies between 0 (for the separable product states) and a maximum of $\log d$ (for the maximally entangled states corresponding to a completely mixed density operator), where d is the dimension of the Hilbert space of the subsystem. A general state of the system can be expressed in term of the Fock states as

$$|\psi\rangle = \sum_{n=0}^{N} c_n(t)\,|n\rangle_a\,|N-n\rangle_b\,, \tag{11}$$

which implies that the mode a has n bosons and the mode b has $N - n$ bosons at the same time, where c_n satisfies the normalizing condition $\sum_{n=0}^{N}|c_n(t)|^2 = 1$.

Using the Fock basis, we have

$$\rho_{ab} = |\psi\rangle\langle\psi| = \sum_{n,m=0}^{N} c_m c_n^* |m\rangle_a |N-m\rangle_{ba}\langle m|_b\langle N-n|. \tag{12}$$

The reduced density operator of mode a is obtained by taking the partial trace with respect to mode b

$$\rho_a = \mathrm{Tr}_b(|\psi\rangle\langle\psi|) = \sum_{n=0}^{N} |c_n(t)|^2 |n\rangle_{aa}\langle n|. \tag{13}$$

From the above expression, we can see that the reduced density operator in the Fock basis is diagonal and the eigenvalues are simply $|c_n(t)|^2$. The entropy of entanglement between the two modes thus reads

$$E(\rho_a) = -\mathrm{Tr}(\rho_a \log \rho_a) = -\sum_{n=0}^{N} |c_n(t)|^2 \log|c_n(t)|^2. \tag{14}$$

Figure 4 pertains to the behavior of the entanglement for the three lowest eigenstates as shown in part b of Figure 1. A distinct change in the behavior of entanglement properties near the anti-crossing points is observed. The ground state entanglement displays a peak exactly at the anti-crossing point $\gamma = 0$ (Fig. 4a). For the first excited state, the entanglement reaches its local maxima near the anti-crossing points $\gamma = 0, \pm 0.045$ (Fig. 4b). For the second excited state, there are five the anti-crossing points shared with other quantum energy levels, $\gamma = 0, \pm 0.045, \pm 0.09$, where the entanglement approaches an extremum (Fig. 4c). Interestingly, two of these anti-crossing points, $\gamma = \pm 0.09$, are very close to the classical bifurcation points. Similarly, Figure 5 shows the influence of the supercritical pitchfork bifurcation on the ground state entanglement in the case of $\gamma = 0$. It is clear that the ground state entanglement displays a peak at a quantum critical point that tends to the corresponding classical bifurcation point $(-\lambda/c = 1)$ as $N \to \infty$. These may be an indicator of the corresponding classical dynamics.

In summary, we have studied the influence of the classical bifurcation behavior on quantum states, including the ground state entanglement and the low excited state entanglement. The system under consideration displays two different types of bifurcations: one is the saddle-node bifurcation and the other the supercritical pitchfork bifurcation. It is shown that the classical bifurcations are closely associated with a topological change in the structure of the corresponding quantum levels. The saddle-node bifurcation is related to the avoided level-crossing of some quantum levels, and the supercritical pitchfork bifurcation is linked to the near degeneracy of some quantum levels. We find that the entanglement of the quantum states involved in the classical bifurcation displays some peaks near the classical bifurcation points. At the same time, the sign of the interaction parameter u can play an important role in determining the structure of the quantum levels. The classical bifurcations are related to the higher part of the quantum levels in the case of positive u, while they are associated with the lower part of the quantum levels in the case of negative u [13,21–24]. Our results are strongly related to similar behaviour in works [11,12]. We note that the supercritical pitchfork bifurcation studied in references [11,12] is related to a structure change of the

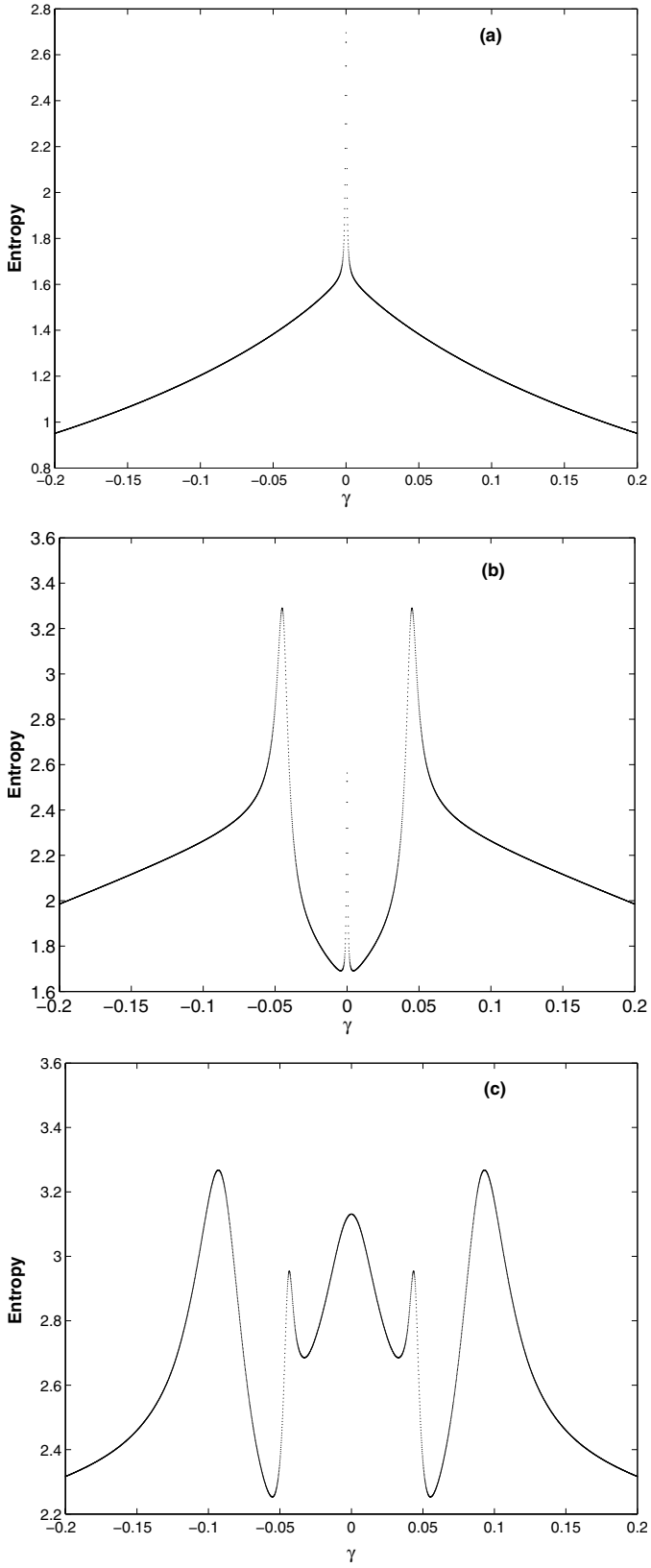

Fig. 4. Von Neumann entropy of the three lowest states of the quantum model $\hat{H}$. (a) The ground state, (b) the first excite state, (c) the second excited state. Other parameters are the same as in Figure 1b.

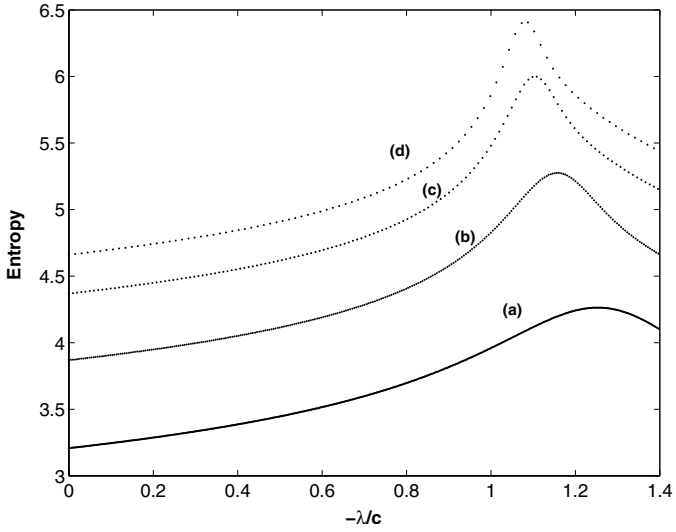

Fig. 5. The dependence of the von Neumann entropy of the ground states for the quantum model $\hat{H}$ on parameter λ/c for (a) $N = 20$, (b) $N = 50$, (c) $N = 100$, (d) $N = 150$.

ground state, while the same bifurcation in reference [13] is linked to a structure change of the highest excited state. These results do not really differ, but instead arise from the same phenomenon, happening in different parts of the spectrum.

This work was supported by the National Natural Science Foundation of China under Grant No. 10575034 and 10275023, and by the Laboratory of Magnetic Resonance and Atomic and Molecular Physics of China under Grant No. T152504.

References

1. M.A. Nielsen, I.L. Chuang, *Quantum Computation and Quantum Communication* (Cambridge University Press, Cambridge, 2000)
2. S. Sachdev, *Quantum Phase Transitions* (Cambridge University Press, Cambridge, 1999)
3. A. Osterloh, L. Amico, G. Falci, R. Fazio, Nature **416**, 608 (2002)
4. T.J. Osborne, M.A. Nielsen, Phys. Rev. A **66**, 032110 (2002)
5. G. Vidal, J.I. Latorre, E. Rico, A. Kitaev, Phys. Rev. Lett. **90**, 227902 (2003)
6. W. Hai, Ya Li, B. Xia, X. Luo, Europhys. Lett. **71**, 28 (2005); W. Hai, G. Chong, Q. Xie, J. Lu, Eur. Phys. J. D **28**, 267 (2004); W. Hai, C. Lee, X. Fang, K. Gao, Physica A **335**, 445 (2004)
7. N. Lambert, C. Emary, T. Brandes, Phys. Rev. Lett. **92**, 073602 (2004)
8. Q. Xie, W. Hai, Eur. Phys. J. D **33**, 265 (2005)
9. L.F. Santos, G. Rigolin, C.O. Escobar, Phys. Rev. A **69**, 042304 (2004)
10. S. Schneider, G.J. Milburn, Phys. Rev. A **65**, 042107 (2002)

11. A.P. Hines, C.M. Dawson, R.H. McKenzie, G.J. Milburn, Phys. Rev. A **70**, 022303 (2004)
12. A.P. Hines, R.H. McKenzie, G.J. Milburn, Phys. Rev. A **71**, 042303 (2005)
13. X.W. Hou, J.H. Chen, B. Hu, Phys. Rev. A **71**, 034302 (2005)
14. A. Micheli, D. Jaksch, J.I. Cirac, P. Zoller, Phys. Rev. A **67**, 013607 (2003)
15. J. Stenger, S. Inouye, D.M. Stamper-Kurn, H.-J. Miesner, A.P. Chikkatur, W. Ketterle, Nature **396**, 345 (1998)
16. J. Williams, R. Walser, J. Cooper, E. Cornell, M. Holland, Phys. Rev. A **59**, 31(R) (1999)
17. F.T. Arecchi, E. Courtens, R. Gilmore, H. Thomas, Phys. Rev. A **6**, 2211 (1972)
18. A. Smerzi, S. Fantoni, S. Giovanazzi, S.R. Shenoy, Phys. Rev. Lett. **79**, 4950 (1997)
19. G.J. Milburn, J. Corney, E.M. Wright, D.F. Walls, Phys. Rev. A **55**, 4318 (1997)
20. C. Lee, W. Hai, L. Shi, X. Zhu, K. Gao, Phys. Rev. A **64**, 053604 (2001); W. Hai, C. Lee, G. Chong, L. Shi, Phys. Rev. E **66**, 026202 (2002); Q. Xie, W. Hai, G. Chong, Chaos **13**, 801 (2003); X. Luo, W. Hai, Chaos **15**, 033702 (2005); Y. Li, W. Hai, J. Phys. A: Math. Gen. **38**, 4105 (2005)
21. O. Zobay, B.M. Garraway, Phys. Rev. A **61**, 033603 (2000)
22. M.E. Kellman, V. Tyng, Phys. Rev. A **66**, 013602 (2002)
23. J. Liu, L. Fu, B.Y. Ou, S.G. Chen, Dae-II Choi, B. Wu, Q. Niu, Phys. Rev. A **66**, 023404 (2002)
24. C. Lee, W. Hai, L. Shi, K. Gao, Phys. Rev. A **69**, 033611 (2004)
25. Z.P. Karkuszewski, K. Sacha, A. Smerzi, Eur. Phys. J. D **21**, 251 (2002)
26. Biao Wu, Jie Liu, Phys. Rev. Lett. **96**, 020405 (2006)
27. A.P. Hines, R.H. McKenzie, G.J. Milburn, Phys. Rev. A **67**, 013609 (2003)
28. A. Søensen, L.-M. Duan, J.I. Cirac, P. Zoller, Nature **409**, 63 (2001)